HHS Public Access

Author manuscript

Arch Biochem Biophys. Author manuscript; available in PMC 2020 May 05.

Published in final edited form as:

Arch Biochem Biophys. 2019 March 15; 663: 192–198. doi:10.1016/j.abb.2019.01.014.

Is alkaline phosphatase biomimeticaly immobilized on titanium able to propagate the biomineralization process?

Marco A. R. Andrade[#,a], **Rafael Derradi**[a], **Ana M. S. Simão**[a], **José Luis Millán**[b], **Ana P. Ramos**[a], **Pietro Ciancaglini**[a], **Maytê Bolean**[a,*]

[a]Departamento de Química, Faculdade de Filosofia, Ciências e Letras de Ribeirão Preto, Universidade de São Paulo, 14040-901 Ribeirão Preto, São Paulo, Brazil

[b]Sanford Burnham Prebys Medical Discovery Institute, La Jolla, California 92037, USA

Abstract

Tissue-nonspecific alkaline phosphatase (TNAP) is a key enzyme in the biomineralization process as it produces phosphate from a number of phospho-substrates stimulating mineralization while it also inactivates inorganic pyrophosphate, a potent mineralization inhibitor. We have previously reported on the reconstitution of TNAP on Langmuir monolayers as well as proteoliposomes. In the present study, thin films composed of dimyristoylphosphatidic acid (DMPA) were deposited on titanium supports by the Langmuir-Blodgett (LB) technique, and we determined preservation of TNAP's phosphohydrolytic activity after incorporation into the LB films. Increased mineralization was observed after exposing the supports containing the DMPA:TNAP LB films to solutions of phospho-substrates, thus evidencing the role of TNAP on the growth of calcium phosphates after immobilization. These coatings deposited on metallic supports can be potentially applied as osteoconductive materials, aiming at the optimization of bone-substitutes integration in vivo.

Graphical Abstract

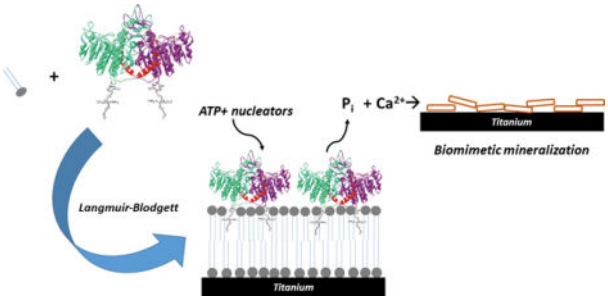

Keywords

Alkaline phosphatase; cell membrane models; Langmuir monolayers; Langmuir-Blodgett films; biomineralization

*Corresponding author: maytebolean@usp.br.
#present address: Universidade Federal de Uberlândia, Rua Ruy Corrêa, Patos de Minas, BR 38702018

Introduction

The osseous tissue is constituted by an inorganic component composed of hydroxyapatite and an organic matrix constituted predominantly of collagen fibers. Like any other metabolic process, osseous histogenesis is regulated by enzymatic pathways from chondro-osteogenic cells, responsible for the control and availability of ions required for the calcification of the osseous matrix (Ca^{2+}, PO_4^{3-}, CO_3^{2-}) or inhibitors of that process (primarily pyrophosphate but also osteopontin, matrix GLA protein) [1–4].

The tissue-nonspecific alkaline phosphatase (TNAP) isozyme is a homodimeric ectoenzyme that releases inorganic phosphate in the extracellular media and controls the extracellular pyrophosphate concentration [3,5]. This enzyme is covalently bound to the external surface of matrix vesicles (MVs) through a glycosylphosphatidylinositol (GPI) hydrophobic anchor [6,7]. MVs are vesicles of 100–300 nm diameter, which are able to bind to the collagen produced by chondro-osteogenic cells and initiate mineralization of the extracellular matrix [8]. These native vesicles contain a nucleational core composed of amorphous calcium phosphate and lipid-calcium-phosphate complexes (CPLXs) responsible for initiation of mineralization [9].

Several techniques can be used for the construction of mimetic models of a cell membrane in order to study its interaction with biological macromolecules. Among them, Langmuir monolayers [10], Langmuir-Blodgett (LB) films [11], and proteoliposomes [12–15] that could mimic the function of MVs, are the most studied. Using these models, natural processes can be mimicked through immobilization of proteins, fibers, and enzymes [16–20], like the biomineralization process, through the nucleation and growth of hydroxyapatite crystals in these templates [13,14,16,21,22].

Langmuir monolayers and LB films are advantageous as membrane models as it is possible to control at molecular level each step of the construction of those templates. The composition (amount and proportion), the number of layers, and polarity of the surface (hydrophobic or hydrophilic depending on the top layer) can be easily regulated by using these techniques [23,24]. The highly organized molecular array at the air-liquid interface is maintained during the monolayer transfer to the solid support, enabling the use of LB films as templates to immobilize enzymes, antibodies or specific ligands, functionalizing the surface for biospecificity [25].

Taking into account the enzymatic diversity and the high complexity of the osseous matrix mineralization, the LB films are a possible option to immobilize and analyze key enzymes involved in ossification, such as TNAP [20,26]. Piatteli et al. [27] immobilized TNAP directly over Ti surfaces by physical adsorption and the results showed that the samples prepared in the presence of the enzyme stimulated the osseous growth around the metallic surface more efficiently than the control samples. The positive results achieved in mineral growth were also achieved *in vitro* by using TNAP-proteoliposomes [14,28].

While the immobilization of TNAP in LB films [26,29] has been reported, there is no study concerning the possible role of the immobilized enzyme in the subsequent mineralization of the biomimetic templates. In the present study, mixed TNAP:Dimiristoylphosphatic acid

(DMPA) Langmuir monolayers were constructed and transferred to Ti supports as LB films in order to evaluate the mineral induction capacity of the immobilized-form of the enzyme.

Experimental Section

Materials:

All solutions were prepared using dust-free ultrapure deionized water from a Milli-Q® system (Surface tension 72.8 $mN.m^{-1}$ and resistivity of 18.2 MΩcm @25°C). Magnesium chloride, *p*-nitrophenylphosphate (pNPP), chloroform, 2-amino-2-methyl-propan-1-ol (AMPOL) were purchased from Sigma Chemical Co. 1,2-dimyristoyl-*sn*-glycero-3-phosphate (DMPA sodium salt) (99+%) was obtained from AVANTI Polar Lipids. Methanol (MeOH, 99+%) and calcium chloride was purchased from J.T. Baker. Calbiosorb was purchased from Merck-Millipore.

Preparation of solubilized TNAP:

TNAP was obtained from osteoblasts primary cultures as previously described by Simão et al.[17]. Briefly, samples of membrane-bound TNAP (0.2 $mg.mL^{-1}$) were solubilized with 1% (w/v, final concentration) polyoxyethylene-9-lauryl ether (polidocanol) for 1h at 25 °C, with constant stirring. After centrifugation at 100000*g* for 1 h, each 1 mL of solubilized TNAP was incubated with 200 mg of Calbiosorb resin for 2 hours at 4 °C with constant stirring in order to remove the polidocanol [30]. The protein concentration was estimated in the presence of 2 wt.% of SDS and bovine serum albumin was used as a standard [31].

Titanium surface preparation:

Titanium discs (13 mm × 1.5 mm – REALUM – Brazil) were used as supports for LB films deposition. The arithmetic roughness of the surfaces, determined by atomic force microscopy, was 32 ± 3 nm. They were cleaned during 15 minutes under ultrasound using a detergent solution, followed by ethyl alcohol and finally with acetone. Before use, they were treated in KH_2PO_4/NaOH 0.10 $mol.L^{-1}$ buffer solution (pH 7.5) containing the non-ionic surfactant Span 20 (4.00×10^{-5} $mol.L^{-1}$) for 5 min., at 65 °C under ultrasound agitation. The supports were then exhaustively washed with deionized water.

Surface pressure (π) vs Surface area (A) Isotherms and Langmuir-Blodgett films:

The π–A isotherms were obtained at 25 ± 2 °C in a 216 cm^2 Langmuir trough (Insight–Brazil) by spreading: (1) 30 μL of 1.0 $mmol.L^{-1}$ DMPA solution dissolved in chloroform/methanol (3:1 v/v), (2) different amount of TNAP aqueous solution, and (3) mixed TNAP:DMPA on pure water or 70 $mmol.L^{-1}$ $CaCl_2$ subphases. Five minutes after the lipids spreading, the surface area was reduced using a movable barrier at 0.42 $mm.s^{-1}$.

In order to investigate the rheological properties of the monolayers, the compressional modulus (Cs^{-1}) was calculated. Cs^{-1} is defined as

$$Cs^{-1} = -A\left(\frac{d\pi}{dA}\right)_T \quad \text{(Eq. 3)}$$

The more compacted the monolayer, the lower its fluidity and consequently the higher is the Cs^{-1} value [32].

The DMPA and DMPA:TNAP monolayers were morphologically analyzed by BAM microscopy (BAM2 Plus-Nanofilm Technologies Germany) equipped with a 10X magnification objective, and incident laser at 53.1 degrees from the surface of the air-liquid interface of a Langmuir KSV-Nima trough (Biolin Scientific), reducing the surface-area with 2 movable barriers at 10 $mm.min^{-1}$.

LB films containing pure DMPA were transferred from the pre-built monolayers, from the emersion of the Ti supports. This ensured a contact of the surfactant polar-head with Ti-surface, along with the hydrophobic tails oriented to the outside of the solid support. LB mixed films of TNAP:DMPA were deposited over this pre-built DMPA film at π = 30 $mN.m^{-1}$ and deposition rate of 0.038 $mm.s^{-1}$, from the immersion of the Ti-modified support. The π was maintained constant at 30 $mN.m^{-1}$ by continuously compressing the monolayer during its transfer to the solid support. The monolayers were stable over this time range as evidenced by π vs time curves (data not shown). The structure of the mixed LB film is illustrated in the Figure 1.

The amount of DMPA and TNAP deposited per LB-layer was estimated using a quartz crystal microbalance (QCM) by the deposition of the monolayers on piezoelectric gold-covered quartz crystal (10 MHz ICM crystals). The changes in oscillation frequencies (Δf) due to the mass deposited are related according to the Sauerbrey equation [33]; $\Delta f = (- (1.1 \times 10^{-6}\ g^{-1}\ cm^2\ s)\ F_0^2\ \Delta m) / A$, where F_0 is the initial frequency, Δm is the deposited mass and A is the electrode area (0.662 cm^2). The transfer ratio is the result of the quotient of the solid support area and the surface compressed area during the transferring of the LB-film to the solid support.

Enzyme kinetics assay:

The phosphohydrolytic activity of TNAP in homogeneous media was estimated continuously through the hydrolysis of the synthetic substrate p-nytrophenylphosphate (pNPP), by spectrophotometry (Agilent/HP 8453) with the aid of quartz cuvettes (1 cm optical length). The enzymatic activity was followed by the changes in the intensity of the UV-Vis absorption band at 410 nm assigned to the formation of *p*-nitrophenolate (pNP^-) (Supporting Information, Figures S1 and S2). The reaction media was a 70 $mmol.L^{-1}$ AMPOL (pH 10.0), 10 $mmol.L^{-1}$ of pNPP, and 2 $mmol.L^{-1}$ of $MgCl_2$ aqueous solutions.

In order to determine the activity of TNAP immobilized onto the LB films deposited on Ti, the supports were incubated in 1.5 mL of the reaction media at a 24-well microplate, and the activity was estimated by UV-vis spectrophotometry [26].

Mineralization assay using TNAP:DMPA mixed LB-films:

The propagation of minerals was evaluated in the presence of a synthetic nucleation complex made of amorphous calcium phosphate (ACP) combined with calcium–phosphate–lipid complexes (PS-CPLX) adapting the procedure described by Genge et al.[9], as described by Simão et al. [14,28]. Briefly, the Ti supports modified with the mixed TNAP:DMPA films

were exposed to 100 μL of synthetic cartilage lymph (SCL) containing PS-CPLX at pH 7.5, 2 mmol.L^{-1} Ca^{2+}, 1 mmol.L^{-1} ATP (phosphate source by TNAP hydrolysis), 104.5 mmol.L^{-1} Na^{+}, 133.5 mmol.L^{-1} Cl^{-}, 63.5 mmol.L^{-1} sucrose, 16.5 mmol.L^{-1} Tris, 12.7 mmol.L^{-1} K^{+}, 5.55 mmol.L^{-1} glucose, 1.83 mmol.L^{-1} HCO_3^{-} and 0.57 mmol.L^{-1} $MgSO_4$ [34], for 6 days at 37°C. Pure DMPA LB films were used as control. Mineral formation was measured by absorbance at 340 nm using a multiwall microplate assay (Sunnyvale, CA) M3 microplate reader system [9,28].

Composition and morphological characterization:

The chemical groups were identified by Fourier-Transform Infrared Spectroscopy (FTIR) coupled to an attenuated total reflectance (ATR) accessory (Shimadzu-IR Prestige-21). The morphology of Ti surfaces modified with the mixed DMPA:TNAP LB films after 6 days of exposure to SCL was investigated by scanning electron microscopy (SEM) using a Zeiss-EVO 50 microscope. The samples were coated with gold before the analysis.

Osteoblasts viability:

The osteoblasts proliferation on the modified Ti surfaces was evaluated through the MTT assay, by the colorimetric analysis of the formazan dye, produced from the tetrazolium salt [3-(4,5-dimethylthiazol-2-yl)-2,5-diphenyl tetra-zolium bromide], a reaction dependent of the NADH reduction, as already described [35]. Briefly, the Ti discs modified with the LB films were incubated at 1.00 mL of culture media (in a 24-well microplate), containing a suspension of 2×10^4 cells, for 3, 7 and 10 days. The absorbance values for each sample were read at 560 and 690 nm, on a Spectronic device (Genesys 2). The cell viability was expressed as a percentage of the average result for each condition as compared with the control.

Results and Discussion

TNAP surface activity provided by salting-out effect

Figure 2 shows the π–A isotherms of TNAP on different subphases, evidencing absence of surface activity of the detergent-free enzyme on water and the adsorption of the enzyme at the interface at high ionic-strength. This phenomena occurs due to the salting-out effect promoted by the $CaCl_2$, similarly to the effect observed to monovalent salts using low-weight proteins [36,37] or even to TNAP monolayers [38]. The C_S^{-1} values does not exceed 50 mN.m^{-1} for the TNAP monolayers (Figure 2 Inset), showing that condensed states [39] (C_S^{-1} higher than 100 mN.m^{-1}) were not achieved for the pure enzyme monolayers. The concentration of 70 mmol.L^{-1} for the subphase was chosen as the standard for the LB-films construction due to a salting-out effect observed using 60 and 80 mmol.L^{-1} $CaCl_2$.

Ca^{2+}-containing subphases diminish the minimum molecular area of DMPA monolayers

Figure 3 shows the π–A isotherms of DMPA. The shape of the isotherm is in agreement with previously reported data [40,41]. The compression of the monolayer was observed in the presence of $CaCl_2$ at the subphase. The presence of divalent cations promotes a diminishment of the electrostatic repulsion from the negatively charged polar heads of DMPA, like already observed for other phosphate-containing lipids [21,22]. The C_S^{-1} values

show that condensed states are achieved at π higher than 12 and 15 for the lipid spreading on water and 70 mmol.L^{-1} $CaCl_2$ subphases, respectively (see insert in Figure 3).

The values of the molecular areas were calculated from the extrapolation of the tangent of the π-A isotherm to the x-axis. The minimum molecular area is the area occupied per lipid molecule at π=30 mN/m, the surface pressure used to the film transference. The choice of a Ca^{2+}-containing salt as subphase lies in the possibility of transferring this ions bound to the DMPA polar head to the LB films, allowing the sequent precipitation of calcium phosphates [21]. The minimum molecular areas in order to achieve the condensed states of the DMPA monolayers in water and 70 mmol.L^{-1} $CaCl_2$ were 61 ± 3 and 56 ± 1 $Å^2$.$molecule^{-1}$, respectively.

Ca^{2+}-containing subphases enhance the amount of DMPA transferred to LB films

The transference of the pure-DMPA monolayers to solid supports was carried out. The LB film deposition ratio was 47 ± 15 and 240 ± 42 ng.$layer^{-1}$, for the subphases containing pure water and aqueous $CaCl_2$ solution, respectively. These deposition ratios were evaluated by QCM measurements (data not shown). The presence of $CaCl_2$ at the subphase diminished the C_S^{-1} of the DMPA monolayer and increased the deposited mass per layer of the LB film, indicating that Ca^{2+} interaction with the DMPA layer.

The salt concentration used in this study was higher than the concentrations generally used for DMPA Langmuir monolayers [41,42]. This high ionic-strength was used in order to co-adsorb TNAP with DMPA (the first present at the interface only through the salting-out effect).

TNAP at air-liquid interface diminishes the fluidity and drastically affects the morphology of DMPA monolayers at Ca^{2+}-containing subphase

The Figure 4A shows the π-A isotherms obtained by changing the quantity of TNAP added to DMPA monolayers. The expansion of the lipid isotherm was higher with the increase of TNAP amount, indicating that more enzyme molecules were present at the air-liquid interface. On the other hand, the C_S^{-1} was diminished by increasing the relative amount of TNAP (Figure 4A Inset), similar to observed in previous studies of alkaline phosphatase and sphingomyelin mixed monolayers [43].

The morphology of the monolayers on the subphase containing 70 mmol.L^{-1} $CaCl_2$ changed drastically due to the TNAP addition to the air-liquid interface (Figure 4B). In the absence of enzyme, there are rounded and micrometric domains that approaches each other by increasing π. It provides a homogeneous monolayer at π = 30 mN.m^{-1}. The achievement of a condensed phase for the monolayers occurs in at π higher than 15 mN.m^{-1}, as evidenced by the C_S^{-1} values higher than 100 mN.m^{-1} (Figure 4A Inset). The presence of dots with higher reflexivity at this π can thus be assigned to condensed domains. that were nearly absent for lower π values (Figure 4B).

The addition of TNAP to the monolayer promoted the adsorption of the enzyme into the DMPA matrix, even at no-compression state (with π = 0), with stretched structures until a homogeneous monolayer at π = 30 mN.m^{-1} (Figure 4B). This could be possibly explained

by the presence of the GPI-anchor to the interface, intensifying the hydrophobic interactions of the apolar tails of DMPA.

There are no significant changes of C_S^{-1} for π higher than 15 mN.m^{-1} to the 1400:1 DMPA:TNAP monolayers (Figure 4A inset), indicating no phase transition. On the other hand, there is a significant change in the morphology of the mixed monolayer by increasing π, as seen in the Figure 4B. This change can be assigned to a self-organization of the monolayer induced by the the presence of TNAP molecules at the interface.

Mixed lipid-enzyme LB bilayers presented a homogeneous coating of Ti surface and TNAP transferred mass differing by changing DMPA:TNAP molar ratio. The quantification of the total mass transferred to the solid supports in the mixed LB films was carried out (Figure 4C). The DMPA+TNAP total mass transferred was reduced by increasing the amount of TNAP present in the monolayers, even lower than the DMPA LB film itself. Even though the quantity of TNAP was higher at the air-liquid interface (by decreasing the DMPA:TNAP molar ratio), the higher fluidity (as shown by the C_S^{-1} values) hindered the enzyme transfer to solid supports. This result is consistent with the diminishment of the C_S^{-1} values with the increase of the TNAP amount, leading to less condensed monolayers (Figure 4A Inset). Similarly, the transfer ratio to the QCM crystals of the mixed DMPA:TNAP monolayers composed of 1430:1, 1000:1 and 670:1 (molar ratios) were 0.61, 0.50 and 0.44, respectively. Thus, the higher amount of TNAP at interface promotes not only diminishment of the C_S^{-1}, but also makes the monolayer transfer less homogeneous, due to lowering of the transfer ratio. Despite the reduction of the total mass, the percentage of TNAP transferred to solid support was higher using lower amount in the monolayers. The Table 1 brings the DMPA +TNAP total mass and the corresponding percentage of TNAP transferred.

While the monolayer containing 1430 molecules of DMPA for each TNAP resulted in the transference of 48 DMPA for each TNAP, the monolayer containing only 670 DMPA for one TNAP molecule gave rise to LB films containing 295 DMPA molecules for TNAP. In other words, for the LB film containing 1430:1 DMPA:TNAP (molar ratio), the composition of the film is 80% (wt.) assigned to TNAP, while for the 670:1 DMPA:TNAP (molar ratio) TNAP is responsible by only 40% (wt.) of the total mass. This result evidences that increased amount of TNAP at the air-liquid interface does not guarantee its transfer do solid supports.

The first DMPA layer constructed over Ti was accomplished with a transfer ratio of 0.5, evidencing the roughness of the Ti surface that promotes heterogeneous LB film over its surface, despite the homogeneity of the DMPA monolayer at π = 30 mN.m^{-1} (Figure 4B). The transfer ratio values of the second layer were all very close to the ideal value of 1 (Table 1), evidencing the homogeneous transfer of the mixed DMPA:TNAP monolayer to the previously-modified Ti surface.

The transferred quantity of TNAP to LB bilayers modulates its phosphohydrolytic activity at the LB-film constructed over the Ti surface

The phosphohydrolytic activity of TNAP immobilized on these LB templates was measured trough the pNPPase activity under optimal conditions. The results are shown in the Table 1.

The TNAP activity is also reduced in the LB films containing higher amount compared to the films containing lower amount of enzyme. Caseli et al. described the reduction of TNAP enzymatic activity at the air-liquid interface induced by aggregation in high surface density regimes [20]. Recently, our group studied the TNAP enzymatic activity using the pendant drop methodology [44]. The results revealed the influence of the surface pressure, or the monolayers organization, in the enzymatic activity. The changes of the active site orientation and its accessibility to the substrate is the main reason assigned to the reduction of activity in higher interfacial concentration of enzyme [19,26,44,45]. The enzymatic activity of TNAP produced by osteoblasts cultured on LB-films with different surface packing and different interfacial Ca^{2+} concentration is also changed [46].

The enzymatic activity was stable as a function of time, similarly to that observed for the phosphohydrolytic activity of TNAP at homogeneous media (Supporting Information, Figures S1 and S2).

DMPA:TNAP bilayer constructed over the Ti surfaces promoted not only a template for mineral growth but also induced a calcium phosphate mineralization

Once TNAP exhibited stable phosphohydrolytic activity immobilized at the LB template composed of DMPA, the mineral formation induction in this heterogeneous media was verified after incubation with SCL buffer. The ATR-FTIR spectra of the mixed LB-films after 6 days of SCL media exposure are shown at Figure 5. All the spectra present a broad band around 3000–3700 cm^{-1}, attributed to the OH group of a possible inorganic phase (assigned to the phosphate precipitation with Ca^{2+}) or due to adsorbed water. [47]. The narrow bands located at 2920 and 2855 cm^{-1}, corresponds to asymmetrical and symmetrical stretching of C-H groups [48], respectively. It is possible to verify an increase in the intensity of the C-H stretching groups for the samples containing TNAP.

The formation of a mineral phosphate phase is evidenced by the narrow band at 1030 cm^{-1} with higher intensity for the LB-films containing TNAP [49]. The ratio between the area of the bands at 1030 cm^{-1} and 1450 cm^{-1} (C-H group scissoring) calculated for the samples containing different amount of TNAP are presented in the Table 2. A maxima corresponding to the higher amount of phosphate formation occurred for the intermediate 1000:1 DMPA:TNAP (molar ratio). Although this sample was not the one that presented the higher TNAP specific activity, it offered the best condition for the mineral growth. Under similar conditions, liposomes harboring anchored TNAP reported as MVs' biomimetic, showed the ability to mineralize [14].

The optimal condition for phosphorylated substrates hydrolysis by TNAP activity is not the best condition to this enzyme induce the mineral formation [28]. The catalytic activity of TNAP is optimum at alkaline conditions and its role at the mineralization process occurs at physiological pH [14,28]. Moreover, an ideal surface density is required to allow the phosphorylated substrate to access the catalytic site of the enzyme [20].

The SEM images of the Ti surfaces modified with the mixed LB films after 6 days of exposure to the SCL media are shown at Figure 6. At absence of TNAP, the control sample (Figure 6A) show a homogeneous surface, while the sample containing TNAP shows

micrometric particles grown over the entire surface (Figure 6B), suggesting that the presence of the enzyme induced a higher mineral formation.

The osteoblasts proliferation over the modified Ti surfaces as a function of time is shown in the Figure 7. The cells viability does not suffer a significant change over the first 10 days of incubation, suggesting that neither the lipid bilayer nor the mixed TNAP/DMPA LB films are toxic to osteoblasts.

Conclusions

The interaction between DMPA and TNAP at the air-liquid interface was studied by means of the Langmuir techniques. The presence of the enzyme changed the packing and the rheological properties of the lipids monolayers. The higher compressibility values in the presence of Ca^{2+} ions allowed the transference of mixed lipids+TNAP films to solid supports. A higher amount of TNAP present in the monolayers hindered its transference to the LB films (– 80% wt.), wich can be assigned to the presence of TNAP in the coatings obtained from monolayers formed by only 11 % of the enzyme. The enzymatic activity was kept and the films containing the lower amount of TNAP presented the higher specific activity. The Ti-coated surfaces were able to induce the phosphate mineral formation by ATP hydrolysis as attested by infrared spectroscopy. The films are not toxic to osteoblasts and present a potential class of materials able to be tested as osteoconductive materials.

Supplementary Material

Refer to Web version on PubMed Central for supplementary material.

ACKNOWLEDGMENT

We thank Fundação de Amparo à Pesquisa do Estado de São Paulo (FAPESP grants 2012/20946–3; 2014/11941-3; 2015/00345-3; 2016/21236-0; 2017/08892-9), Coordenação de Aperfeiçoamento de Pessoal de Nível Superior - Brasil (CAPES) - Finance Code 001 and Conselho Nacional de Desenvolvimento Científico e Tecnológico (CNPq) for the financial support given to our laboratory. The authors also thank the Professor Bernhard Gross Polymer Group (Instituto de Física de São Carlos – USP) for access to the BAM apparatus.

REFERENCES

[1]. Hessle L, Johnson KA, Anderson HC, Narisawa S, Sali A, Goding JW, et al., Tissue-nonspecific alkaline phosphatase and plasma cell membrane glycoprotein-1 are central antagonistic regulators of bone mineralization, Proc. Natl. Acad. Sci. U. S. A 99 (2002) 9445–9. doi:10.1073/pnas.142063399. [PubMed: 12082181]

[2]. Bollen M, Gijsbers R, Ceulemans H, Stalmans W, Stefan C, Nucleotide pyrophosphatases/phosphodiesterases on the move, Crit. Rev. Biochem. Mol. Biol 35 (2000) 393–432. 10.1080/10409230091169249. [PubMed: 11202013]

[3]. Balcerzak M, Hamade E, Zhang L, Pikula S, Azzar G, Radisson J, et al., The roles of annexins and alkaline phosphatase in mineralization process, Acta Biochim. Pol 50 (2003)(4)1019–38. doi:0350041019. [PubMed: 14739992]

[4]. Wang W, Xu J, Du B, Kirsch T, Role of the Progressive Ankylosis Gene (ank) in Cartilage Mineralization, Mol. Cell. Biol 25 (2005) 312–323. doi:10.1128/MCB.25.1.312-323.2005. [PubMed: 15601852]

[5]. Millán JL, Mammalian Alkaline Phosphatases, Wiley-VCH Verlag GmbH & Co. KGaA, Weinheim, FRG, (2006). doi:10.1002/3527608060.

[6]. Low MG and Saltiel AR, Structural and functional roles of glycosyl-phosphatidylinositol in membranes, Science 239 (1988) 268–275. doi:10.1126/science.3276003. [PubMed: 3276003]

[7]. Ikezawa H, Glycosylphosphatidylinositol (GPI)-Anchored Proteins, Biol. Pharm. Bull 25 (2002) 409–417. 10.1248/bpb.25.409. [PubMed: 11995915]

[8]. Bottini M, Mebarek S, Anderson KL, Strzelecka-Kiliszek A, Bozycki L, Simão AMS, et al., Matrix vesicles from chondrocytes and osteoblasts: Their biogenesis, properties, functions and biomimetic models, Biochim. Biophys. Acta - Gen. Subj 1862 (2018) 532–546. doi:10.1016/j.bbagen.2017.11.005. [PubMed: 29108957]

[9]. Genge BR, Wu LNY, Wuthier RE, In vitro modeling of matrix vesicle nucleation: Synergistic stimulation of mineral formation by annexin A5 and phosphatidylserine, J. Biol. Chem 282 (2007) 26035–26045. doi:10.1074/jbc.M701057200. [PubMed: 17613532]

[10]. Brockman H, Lipid monolayers : why use half a membrane interactions to characterize protein-membrane interactions? Curr. Opin. Struct. Biol 9 (1999) (4) 438–43. doi:10.1016/S0959-440X(99)80061-X [PubMed: 10449364]

[11]. Blodgett KB, Films Built by Depositing Successive Monomolecular Layers on a Solid Surface, J. Am. Chem. Soc 57 (1935) 1007–1022. doi:10.1021/ja01309a011.

[12]. Bolean M, Simão AMS, Favarin BZ, Millán JL, Ciancaglini P, Thermodynamic properties and characterization of proteoliposomes rich in microdomains carrying alkaline phosphatase., Biophys. Chem 158 (2011) 111–8. doi:10.1016/j.bpc.2011.05.019. [PubMed: 21676530]

[13]. Bolean M, Simão AMS, Barioni MB, Favarin BZ, Sebinelli HG, Veschi EA, Janku TAB, Bottini M, Hoylaerts MF, Itri R, Millán JL, Ciancaglini P, Biophysical aspects of biomineralization. Biophys Rev 9 (2017) 747–760. doi: 10.1007/s12551-017-0315-1. [PubMed: 28852989]

[14]. Simão AMS, Bolean M, Favarin BZ, Veschi EA, Tovani CB, Ramos AP, Bottini M, Buchet R, Millán JL, Ciancaglini P, Lipid microenvironment affects the ability of proteoliposomes harboring TNAP to induce mineralization without nucleators. J Bone Miner Metab (2018) doi: 10.1007/s00774-018-0962-8. [Epub ahead of print]

[15]. Itel F, Skovhus TJ, Städler B, Matrix Vesicles-Containing Microreactors as Support for Bonelike Osteoblasts to Enhance Biomineralization, ACS Appl Mater Interfaces 10 (2018) 30180–30190. doi: 10.1021/acsami.8b10886. [PubMed: 30113809]

[16]. Simão AMS, Yadav MC, Ciancaglini P, Millán JL, Proteoliposomes as matrix vesicles ‘ biomimetics to study the initiation of skeletal mineralization Proteoliposomes as matrix vesicles ‘ biomimetics to study the initiation of skeletal mineralization, Brazilian J. Med. Biol. Res 43 (2010) 234–241. doi: 10.1590/S0100-879X2010007500008.

[17]. Simão AMS, Yadav MC, Narisawa S, Bolean M, Pizauro JM, Hoylaerts MF, et al., Proteoliposomes harboring alkaline phosphatase and nucleotide pyrophosphatase as matrix vesicle biomimetics, J. Biol. Chem 285 (2010) 7598–7609. doi:10.1074/jbc.M109.079830. [PubMed: 20048161]

[18]. Petrigliano A, Tronin A, Nicolini C, Deposition and enzymatic activity of Langmuir-Blodgett films of alkaline phosphatase, Thin Solid Films 284–285 (1996) 752–756. 10.1016/S0040-6090(95)08438-X

[19]. Caseli L, Masui DC, Furriel RPM, Leone FA, Zaniquelli MED, Influence of the glycosylphosphatidylinositol anchor in the morphology and roughness of Langmuir–Blodgett films of phospholipids containing alkaline phosphatases, Thin Solid Films 515 (2007) 4801–4807. 10.1016/j.tsf.2006.11.044.

[20]. Caseli L, Furriel RPM, de Andrade JF, Leone FA, Zaniquelli MED, Surface density as a significant parameter for the enzymatic activity of two forms of alkaline phosphatase immobilized on phospholipid Langmuir-Blodgett films, J. Colloid Interface Sci 275 (2004) 123–30. doi:10.1016/j.jcis.2004.01.081 [PubMed: 15158389]

[21]. de Souza ID, Cruz MAE, de Faria AN, Zancanela DC, Simão AMS, Ciancaglini P, et al., Formation of carbonated hydroxyapatite films on metallic surfaces using dihexadecyl phosphate-LB film as template., Colloids Surf. B. Biointerfaces 118 (2014) 31–40. doi:10.1016/j.colsurfb.2014.03.029. [PubMed: 24727116]

[22]. Cruz MAE, Ruiz GCM, Faria AN, Zancanela DC, Pereira LS, Ciancaglini P, et al., Calcium carbonate hybrid coating promotes the formation of biomimetic hydroxyapatite on titanium surfaces, Appl. Surf. Sci 370 (2016) 459–468. doi:10.1016/j.apsusc.2015.12.250.

[23]. Gong K, Feng SS, Go ML, Soew PH, Effects of pH on the stability and compressibility of DPPC/cholesterol monolayers at the air–water interface, Colloids Surfaces A Physicochem. Eng. Asp 207 (2002) 113–125. doi:10.1016/S0927-7757(02)00043-2.

[24]. Gonçalves da Silva AM, Romão RIS, Mixed monolayers involving DPPC, DODAB and oleic acid and their interaction with nicotinic acid at the air-water interface., Chem. Phys. Lipids 137 (2005) 62–76. doi:10.1016/j.chemphyslip.2005.06.004. [PubMed: 16095583]

[25]. Girard-Egrot AP, Godoy S, Blum LJ, Enzyme association with lipidic Langmuir-Blodgett films: interests and applications in nanobioscience., Adv. Colloid Interface Sci 116 (2005) 205–25. doi:10.1016/j.cis.2005.04.006. [PubMed: 16181605]

[26]. Caseli L, Zaniquelli MED, Furriel RPM, Leone FA, Enzymatic activity of alkaline phosphatase adsorbed on dimyristoylphosphatidic acid Langmuir-Blodgett films, Colloids Surfaces B Biointerfaces 25 (2002) 119–128. doi:10.1016/S0927-7765(01)00302-2.

[27]. Piattelli A, Scarano A, Corigliano M, Piattelli M, Effects of alkaline phosphatase on bone healing around plasma-sprayed titanium implants: A pilot study in rabbits, Biomaterials 17 (1996) 1443–1449. doi:10.1016/0142-9612(96)87288-7. [PubMed: 8830973]

[28]. Simão AMS, Bolean M, Hoylaerts MF, Millán JL, Ciancaglini P, Effects of pH on the production of phosphate and pyrophosphate by matrix vesicles' biomimetics., Calcif. Tissue Int 93 (2013) 222–32. doi: 10.1007/s00223-013-9745-3. [PubMed: 23942722]

[29]. Caseli L, Masui DC, Furriel RPM, Leone FA, Zaniquelli MED, Incorporation conditions guiding the aggregation of a glycosylphosphatidyl inositol (GPI)-anchored protein in Langmuir monolayers, Colloids Surf. B. Biointerfaces 46 (2005) 248–54. doi: 10.1016/j.colsurfb.2005.11.007 [PubMed: 16356698]

[30]. Camolezi FL, Daghastanli KRP, Magalhães PP, Pizauro JM, Ciancaglini P, Construction of an alkaline phosphatase–liposome system: a tool for biomineralization study, Int. J. Biochem. Cell Biol 34 (2002) 1091–1101. 10.1016/S1357-2725(02)00029-8. [PubMed: 12009304]

[31]. Hartree EF, Determination of protein: a modification of the Lowry method that gives a linear photometric response., Anal. Biochem 48 (1972) 422–427. doi:10.1016/0003-2697(72)90094-2. [PubMed: 4115981]

[32]. Vollhardt D, Fainerman VB, Progress in characterization of Langmuir monolayers by consideration of compressibility, Adv. Colloid Interface Sci 127 (2006) 83–97. doi:10.1016/j.cis.2006.11.006. [PubMed: 17208192]

[33]. Sauerbrey G, Verwendung von Schwingquarzen zur Wägung dünner Schichten und zur Mikrowägung, Zeitschrif Für Phys 155 (1959) 206–222.

[34]. Wuthier RE, Electrolytes of isolated epiphyseal chondrocytes, matrix vesicles, and extracellular fluid, Calcif. Tissue Res 23 (1977) 125–133. doi:10.1007/BF02012777. [PubMed: 890549]

[35]. Mosmann T, Rapid colorimetric assay for cellular growth and survival: Application to proliferation and cytotoxicity assays, J. Immunol. Methods 65 (1983) 55–63. doi:10.1016/0022-1759(83)90303-4. [PubMed: 6606682]

[36]. Thakur G, Wang C, Leblanc RM, Surface Chemistry and in Situ Spectroscopy of a Lysozyme Langmuir Monolayer, Langmuir 24 (2008) 4888–4893. doi:10.1021/la703893m. [PubMed: 18355099]

[37]. Miñones Conde M, Conde O, Trillo JM, Miñones J, How to obtain a well-spread monolayer of lysozyme at the air/water interfaces, J. Colloid Interface Sci 361 (2011) 351–360. doi:10.1016/j.jcis.2011.04.066. [PubMed: 21641610]

[38]. Caseli L, Masui DC, Furriel RPM, Leone FA, Zaniquelli MED, Orbulescu J, et al., Rat osseous plate alkaline phosphatase as Langmuir monolayer--an infrared study at the air-water interface, J. Colloid Interface Sci 320 (2008) 476–482. doi:10.1016/j.jcis.2008.01.043. [PubMed: 18280491]

[39]. Davies JT, Rideal EK, Interfacial Phenomena, 66 (1963) 453–453. 10.1002/bbpc.19620660515

[40]. Wu F, Gericke A, Flach CR, Mealy TR, Seaton BA, Mendelsohn R, Domain structure and molecular conformation in annexin V/1,2-dimyristoyl-sn-glycero-3-phosphate/Ca2+ aqueous

monolayers: a Brewster angle microscopy/infrared reflection-absorption spectroscopy study., Biophys. J 74 (1998) 3273–3281. doi:10.1016/S0006-3495(98)78034-8. [PubMed: 9635781]

[41]. Ramos AP, Nobre TM, Montoro LA, Zaniquelli MED, Calcium carbonate particle growth depending on coupling among adjacent layers in hybrid LB/LbL films., J. Phys. Chem. B 112 (2008) 14648–54. doi:10.1021/jp8023793. [PubMed: 18774855]

[42]. Caseli L, Nobre TM, Ramos AP, Monteiro DS, Zaniquelli MED, The Role of Langmuir Monolayers to Understand Biological Events, ACS Symp. Ser 1215 (2015) 65–88. doi:10.1021/bk-2015-1215.ch004.

[43]. Wang J, Sun R, Influence of alkaline phosphatase on phase state of the SM monolayers at the air-water interface, Colloids Surfaces A Physicochem. Eng. Asp 489 (2016) 136–141. doi:10.1016/j.colsurfa.2015.10.040.

[44]. Andrade MAR, Favarin B, Derradi R, Bolean M, Simão AMS, Millán JL, et al., Pendant-drop method coupled to ultraviolet-visible spectroscopy : a useful tool to investigate interfacial phenomena, Colloids Surfaces A Physicochem. Eng. Asp 504 (2016) 305–311. doi:10.1016/j.colsurfa.2016.05.085.

[45]. Favarin BF, Andrade MAR, Bolean M, Simão AMS, Ramos AP, Hoylaerts MF, et al., Effect of the presence of cholesterol in the interfacial microenvironment on the modulation of the alkaline phosphatase activity during in vitro mineralization, Colloids Surfaces B Biointerfaces 155 (2017) 466–476. doi:10.1016/j.colsurfb.2017.04.051. [PubMed: 28472750]

[46]. de Faria AN, Cruz MAE, Ruiz GCM, Zancanela DC, Ciancaglini P, Ramos AP, Different compact hybrid Langmuir-Blodgett-film coatings modify biomineralization and the ability of osteoblasts to grow, J. Biomed. Mater. Res. Part B Appl. Biomater 3 (2018) 1–11. doi:10.1002/jbm.b.34069.

[47]. Meejoo S, Maneeprakorn W, Winotai P, Phase and thermal stability of nanocrystalline hydroxyapatite prepared via microwave heating, Thermochim. Acta 447 (2006) 115–120. doi:10.1016/j.tca.2006.04.013.

[48]. Wang SH, Griffiths PR, Resolution enhancement of diffuse reflectance i.r. spectra of coals by Fourier self-deconvolution. 1. C-H stretching and bending modes, Fuel 64 (1985) 229–236. doi:10.1016/0016-2361(85)90223-6.

[49]. Han JK, Song HY, Saito F, Lee BT, Synthesis of high purity nano-sized hydroxyapatite powder by microwave-hydrothermal method, Mater. Chem. Phys 99 (2006) 235–239. doi:10.1016/j.matchemphys.2005.10.017.

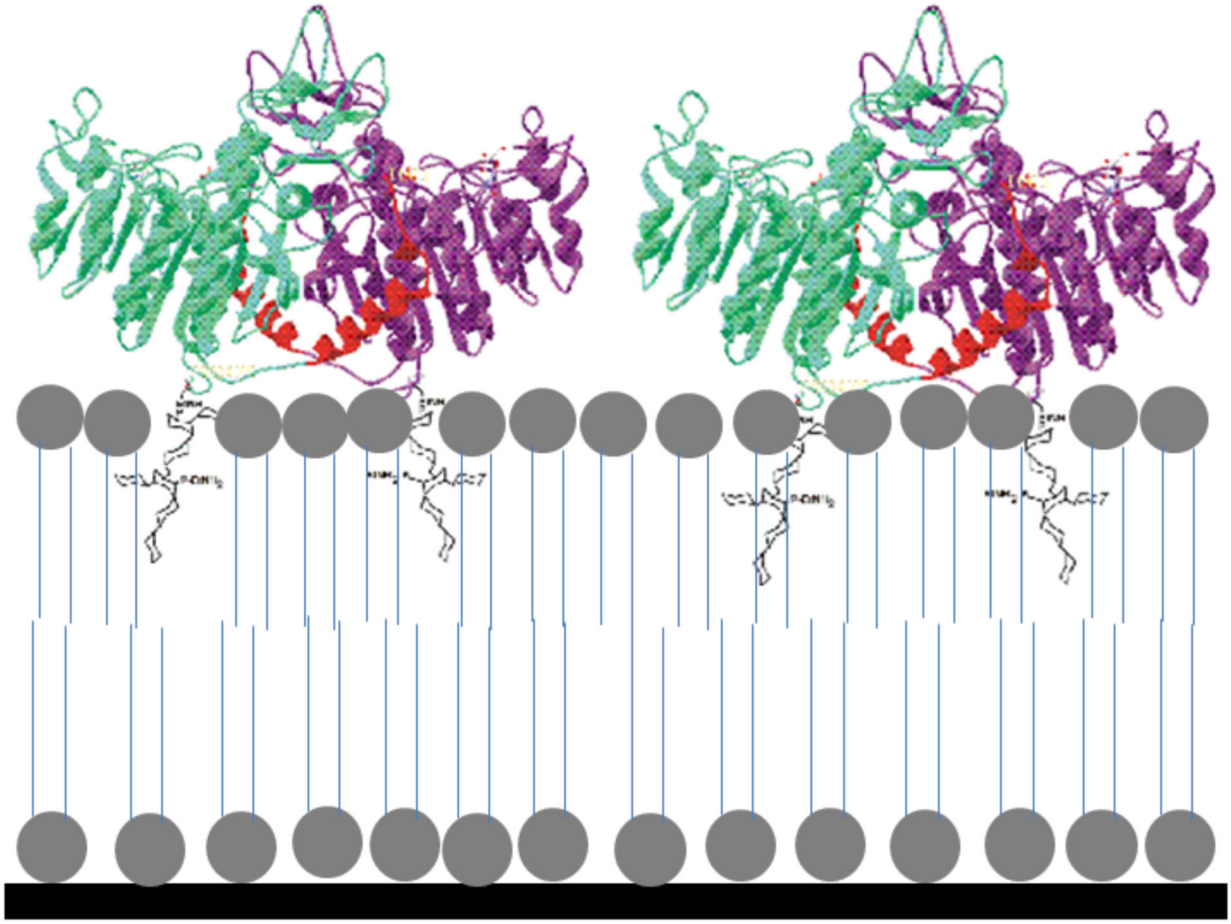

Figure 1:
Schematic representation of the DMPA-TNAP LB film.

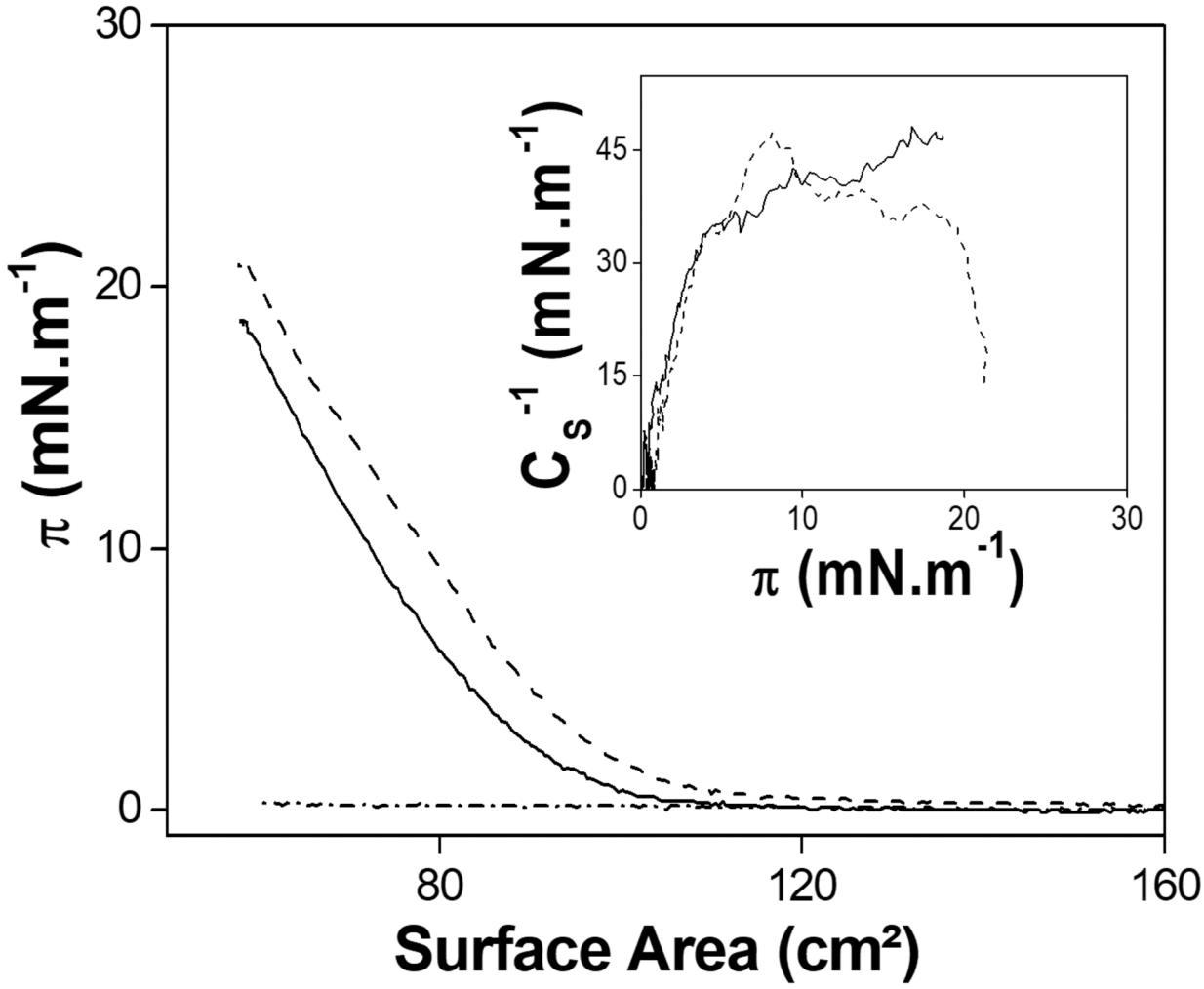

Figure 2.

π-A isotherms of TNAP (5.7 μg) spread on water (dash-dotted line), 60 and 80 mmol.L^{-1} $CaCl_2$ (solid and dashed, respectively). Inset: C_S^{-1} as a function of **π** for the monolayers obtained on $CaCl_2$ subphases.

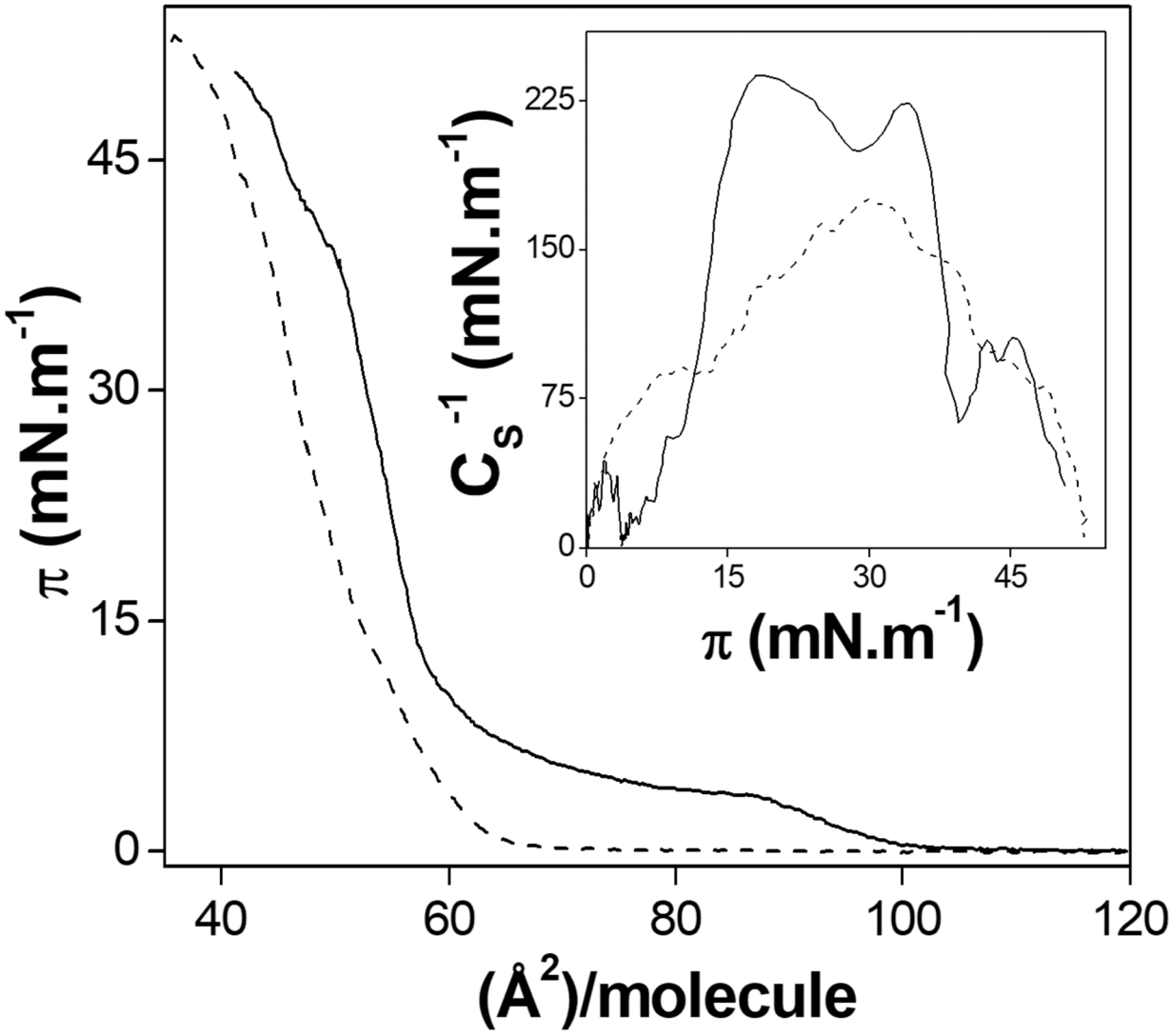

Figure 3.

DMPA π–A isotherms in water (solid) and 70 mmol.L^{-1} $CaCl_2$ solution (dashed line) subphases. Inset: C_S^{-1} as a function of π for each monolayer.

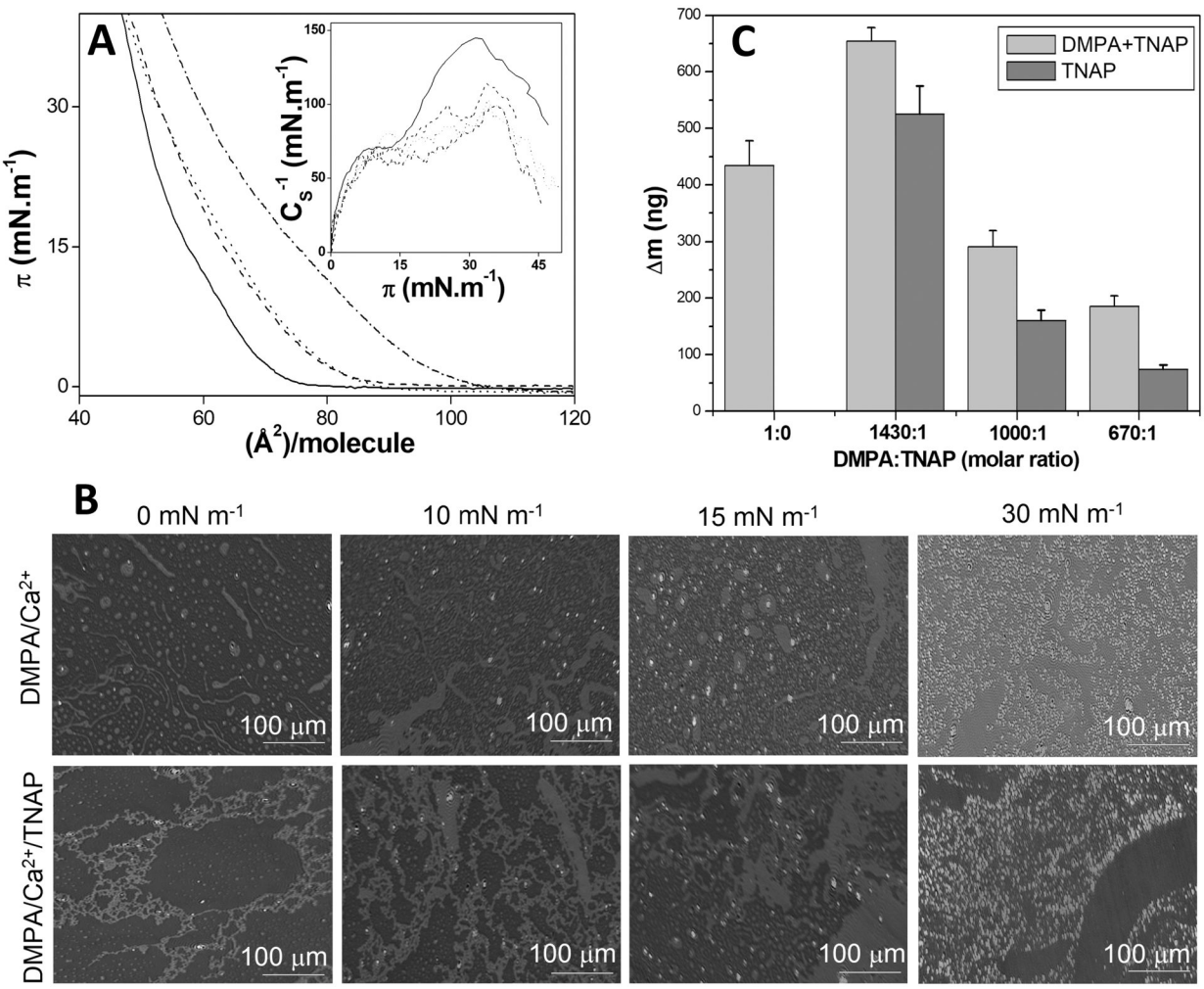

Figure 4. (A)

π–A isotherms of pure DMPA (solid line) and DMPA:TNAP 1430:1 (dashed line), 1000:1 (dotted line) and 670:1 (dashed-dotted line) (molar ratios) on 70 mmol.L^{-1} $CaCl_2$ aqueous solution as subphase. Insert: C_S^{-1} as a function of **π** for each isotherm. **(B)** BAM microscopy images of DMPA and DMPA:TNAP 1430:1 (molar ratio) monolayers at different **π** values on 70 mmol.L^{-1} $CaCl_2$ aqueous solution as subphase. **(C)** The mass of DMPA+TNAP LB films deposited onto the QCM surface and TNAP obtained by subtracting the theoretical DMPA mass using the minimum molecular area from the isotherms as a function of DMPA:TNAP molar ratio.

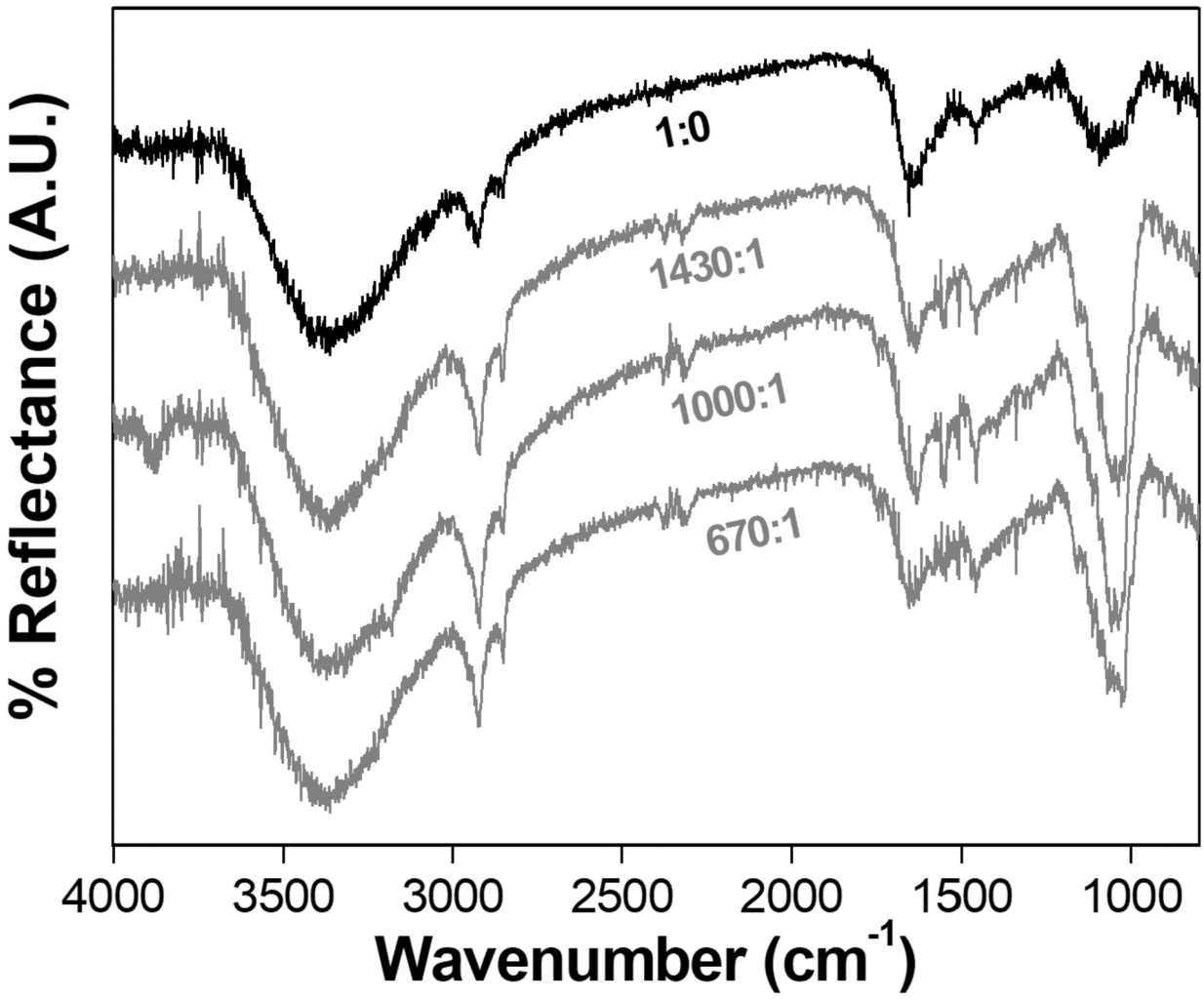

Figure 5.
ATR-FTIR spectra of the Ti surfaces modified with DMPA:TNAP LB films after 6 days of exposure to SCL media.

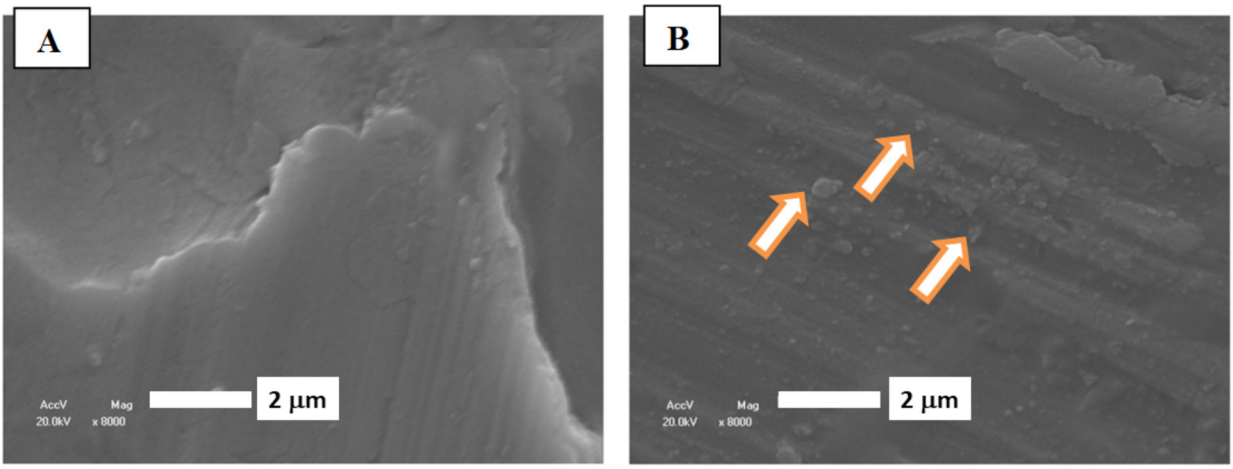

Figure 6.

SEM images of the Ti surfaces modified with DMPA (A) and DMPA:TNAP (B) bilayer transferred from the monolayer containing 1000:1 DMPA:TNAP (molar ratio), after exposure to SCL media for 6 days. Arrows in (B) indicated micrometric particles.

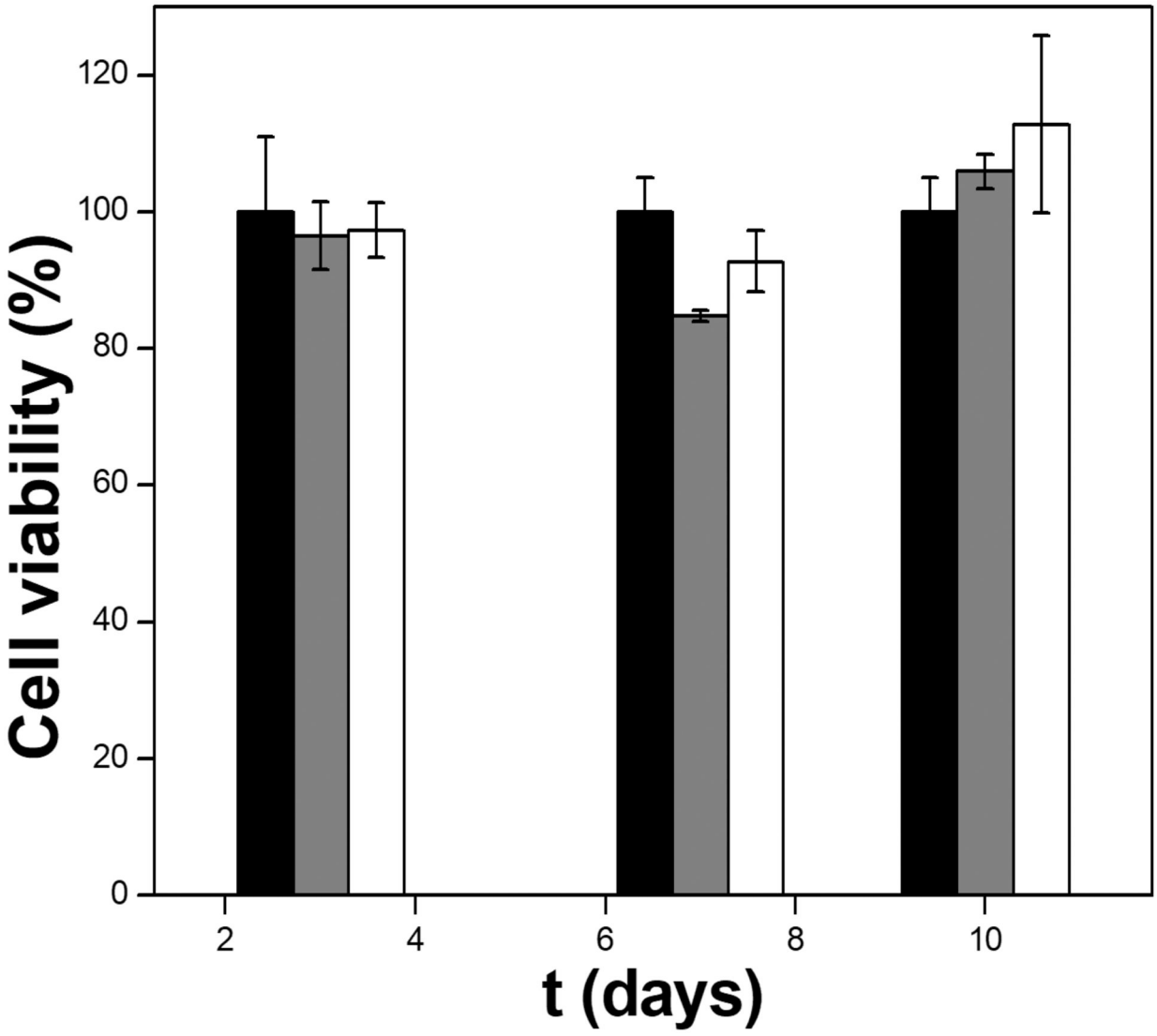

Figure 7.

Cell viability as a function of time obtained for osteoblasts cultured in the presence of unmodified Ti discs as controls (black), modified samples containing DMPA (grey) and 1000:1 DMPA:TNAP (molar ratio) LB bilayers (white) bars.

Table 1:

The total mass of DMPA+TNAP deposited onto the QCM surface and TNAP present in the LB films transferred from monolayers with different lipid:protein molar ratio, and the enzymatic activity for the respective compositions. The mass of TNAP was calculated by subtraction the mass of DMPA calculated from the minimum area of the corresponding π-A isotherms

DMPA:TNAP (molar ratio)	% of TNAP (wt.)	DMPA:TNAP (molar ratio)	Total mass (ng)	TNAP (ng)	% of TNAP (wt.)	Specific activity (U.mg $^{-1}$)	Transfer Ratio
in the monolayers		***in the Langmuir-Blodgett films***					
1430:1	11	48:1	655±20	525±50	80	1.3×10^{-3}	0.94
1000:1	17	157:1	291±30	161±18	55	9.3×10^{-3}	0.98
670:1	25	295:1	186±20	74±8	40	21×10^{-3}	1.07

Table 2:

Ratio between the areas of the bands at 1030 and 1450 cm^{-1}.

DMPA:TNAP	1030/1450
1430:1	1.9±0.2
1000:1	2.9±0.4
670:1	1.9±0.2